Study of the Shubnikov-de Haas Effect. Determination of the Fermi Surfaces in Graphite

D. E. SOULE
Research Laboratory, Carbon Products Division of Union Carbide, Parma, Ohio

AND

J. W. MCCLURE* AND L. B. SMITH†
Parma Research Laboratory of Union Carbide, Parma, Ohio

(Received 21 October 1963)

Measurements of the oscillatory magnetoresistance of a high-quality graphite single crystal were made for all angles θ between the magnetic field and the c axis, for magnetic fields up to 24 kG, and for temperatures from 1.22 to 4.22°K. The results were analyzed by a least-squares fitting to a generalized Landau formula. Oscillations due to electrons were observed for all orientations (including $\mathbf{H}\perp\mathbf{c}$, where the amplitude dropped by a factor 10^5), proving that the electron Fermi surfaces are *closed*. Although oscillations due to holes were not observed beyond $\theta\simeq 84°$, indirect arguments show that the hole Fermi surfaces are also closed. Both electron and hole surfaces are elongated along the c axis and have anisotropy ratios of 12.1 ± 1.4 and about 17, respectively. The electron surface is approximately ellipsoidal, whereas the hole surface is similar except for extended ends giving it a diamond-like shape. The results are consistent with a moderate degree of trigonal asymmetry about the c axis. Comparison between the electron density found from the volume of the electron Fermi surfaces and that determined previously from the nonoscillatory galvanomagnetic data confirms the theoretical prediction that there are four electron Fermi surfaces in the Brillouin zone. More indirect arguments show that there are two hole surfaces. Consideration of the size and location of these surfaces along the six zone edges parallel to the c axis leads to a new determination of $\Delta\simeq -0.12$ eV for the band parameter which represents the difference of potential between the two types of atomic sites in the graphite lattice. Analysis of the temperature and magnetic field dependence of the oscillatory amplitude yields effective mass values in the basal plane of $(0.039\pm 0.001)m_0$ for electrons and $(0.057\pm 0.002)m_0$ for holes. These masses show an orientation dependence that is consistent with the derived Fermi surface anisotropies. The large amplitude and asymmetric shape of the oscillations in the magnetoconductivity, measured for $\mathbf{H}\|\mathbf{c}$ at 1.26 and 4.22°K, are accurately described by the theory of Adams and Holstein. However, there is an unexplained monotonic variation with magnetic field in the total magnetoconductivity. The effective change in temperature due to collision broadening ΔT is about 5 times greater than that estimated from the conductivity relaxation time. This discrepancy in ΔT is qualitatively explained and is related directly to the fact, established from the data of Berlincourt and Steele, that the ΔT found from magnetoresistance oscillations is greater than that found from susceptibility oscillations on the same sample.

I. INTRODUCTION

THE Shubnikov-de Haas effect,[1] an oscillatory dependence of the electrical resistivity on the magnetic field, is directly related to the de Haas-van Alphen effect. Both are produced by the oscillation of the density of states at the Fermi level caused by the quantization of electron energy levels in the presence of a magnetic field.[2,3] The oscillations are periodic in inverse field and the period P is related to the extreme cross section of the Fermi surface A_m perpendicular to the applied magnetic field by the Onsager[4]-Lifshitz[5] relation

$$P=2\pi e/c\hbar A_m. \tag{1.1}$$

The period, therefore, depends upon the relative orientation of the magnetic field with respect to the crystallographic axes so that the shape of the Fermi surface may be deduced from such an orientation study. Although there has been extensive work determining Fermi surfaces using the de Haas-van Alphen effect,[6] somewhat less effort[7] has been spent using the Shubnikov-de Haas effect for this purpose.

The present investigation is a continuation of previous work[8] on the oscillatory galvanomagnetic effects in high-quality graphite single crystals at 4.2°K with the magnetic field parallel to the hexagonal c axis. This investigation represents the first study of the *entire* highly anisotropic Fermi surfaces in graphite. The study was extended to all angles between the magnetic field **H** and the c axis (defined as θ) in the temperature range from 1.22 to 4.22°K. Oscillations were observed at all values of θ, including the most critical orientation of **H** perpendicular to **c**, where the amplitude of the oscillations was extremely small. In fact, the principal reason why the magnetoresistance was used in this study was

* Present address: Department of Physics, University of Oregon, Eugene, Oregon.
† Present address: Computation Center, Stanford University, Palo Alto, California.
[1] L. Shubnikov and W. J. de Haas, Comm. Phys. Lab. Univ. Leiden, No. 207a (1930).
[2] R. Peierls, Z. Physik **81**, 186 (1933).
[3] L. D. Landau; see Appendix of D. Shoenberg, Proc. Roy. Soc. (London) **A170**, 341 (1939).
[4] L. Onsager, Phil. Mag. **43**, 1006 (1952).
[5] I. M. Lifshitz; see notes added in proof of D. Shoenberg, *Progress in Low-Temperature Physics* (North-Holland Publishing Company, Amsterdam, 1957), Vol. II, p. 226.
[6] D. Shoenberg, Phil. Trans. Roy. Soc. London **A245**, 1 (1952).
[7] See literature cited in Ref. 8 and in A. H. Kahn and H. P. R. Frederikse, *Solid State Physics* (Academic Press, Inc., New York, 1959), Vol. IX, p. 257.
[8] D. E. Soule, Phys. Rev. **112**, 708 (1958).

that it afforded a very sensitive and accurate method for observing the oscillations at all orientations.

The determination of the Fermi surface shape in graphite has added importance because it has been the subject of controversy. The de Haas-van Alphen effect showed two periods.[6] As all the measurements were for small θ, two interpretations of the results were possible: (1) The periods correspond to the maximum and minimum cross sections of one surface which is open in the direction of the c axis,[4,9] or (2) the periods correspond to the maximum cross sections of two closed surfaces which are elongated along the c axis.[6,10] Both interpretations were given theoretical support. The Sloncewski-Weiss model[11] (hereafter referred to as SW), which expresses the most general behavior of the energy in the neighborhood of the Fermi level, can give either possibility (1) or (2) by a suitable choice of parameters. Haering and Wallace[12] reasoned that the observed value of the steady magnetic susceptibility could be understood only if the main resonance integral between planes γ_1 were very small (<0.005 eV). This assumption, together with the values of the de Haas-van Alphen periods, led to interpretation (1). Haering and Wallace obtained agreement with Kinchin's measured Hall coefficient,[13] but they could not account for later galvanomagnetic[14] and cyclotron resonance[15] measurements which indicated that both electrons and holes were present. Further, they did not obtain agreement with the measured de Haas-van Alphen effective masses.[6,8]

On the other hand, a choice of parameters based on interpretation (2) could account for both the de Haas-van Alphen periods and masses.[10] This work led to theoretical Fermi surface anisotropy ratios (ratio of length in the c direction to width in the a direction) in the range 11 to 13. Further agreement with this view was obtained by an analysis of the cyclotron resonance[16] and the nonoscillatory galvanomagnetic results.[14,17] More recently it has been shown that the steady magnetic susceptibility can also be explained by using interpretation (2).[18] From the cyclotron resonance results, the electron was found to have a smaller effective mass than the hole. From the de Haas-van Alphen type results, the oscillatory term with the largest period was associated with the smaller mass, thereby identifying the Fermi surface with the smallest cross section as that due to electrons.

Since the above arguments were indirect, it was felt important to make a *direct* experimental determination of the Fermi surface shape by means of the Shubnikov-de Haas effect. A discussion of this work constitutes the first part of the paper. As the observed oscillatory structure was complicated by the interference of the two components (electron and hole), a least-squares fitting to a two-carrier "generalized Landau formula" was performed on an electronic computer. At high θ, the electron term could be seen alone, since the hole term was damped below the detectable level. The results discussed in Sec. III show that the electron and hole surfaces are *closed*, proving interpretation (2). The anisotropy ratios were found to be 12.1 and approximately 17, respectively. This information supports the previous conclusion, based upon the equality of carrier concentration[8,14,17] and effective mass evaluation,[8] that the carriers contributing to the oscillatory component of these galvanomagnetic effects represent the major part of the Fermi surfaces. The shape of the electron surface is approximately ellipsoidal whereas that of the hole is roughly "diamond-shaped."

Not only does the extension of the range of the experiment provide the first direct determination of the Fermi surface shape in graphite, but it also provides some of the largest and most asymmetrical Shubnikov-de Haas oscillations observed to date. Thus, a strong test is provided for recent theories of the effect, which constitutes the second part of the paper. A detailed study was made of the magnetoconductivity tensor at 1.26 and 4.22°K, for **H** parallel to **c**. Although the Onsager-Lifshitz relation is satisfactory for the period behavior, and the susceptibility oscillations are well described by the Landau[3] and Lifshitz-Kosevitch[19] theories, there has been disagreement between theories in the literature concerning the amplitude and shape of the magnetoresistivity oscillations. In addition to the period variation, all theories also agree on the thermal damping factor which describes the dependence of the amplitude of the oscillation upon temperature. This factor, which was first derived by Landau, is

$$\Omega = u/\sinh u, \tag{1.2}$$

where $u = 2\pi^2 kT/\Delta E$, T is the temperature and $\Delta E = \hbar eH/m^* c$, the spacing between energy levels, where m^* here is an orbital effective mass. The early calculations by Titeica,[20] Davydov and Pomeranchuk,[21] and Zilberman[22] used an intuitive diffusion-like method. Although later calculations by density matrix methods[23,24] gave results that disagreed with these, a more rigorous density matrix calculation by Adams and Holstein[25]

[9] D. Shoenberg, Ref. 5, p. 259.
[10] J. W. McClure, Phys. Rev. **108**, 612 (1957).
[11] J. C. Slonczewski and P. R. Weiss, Phys. Rev. **109**, 272 (1958).
[12] R. R. Haering and P. R. Wallace, Phys. Chem. Solids **3**, 253 (1957).
[13] G. H. Kinchin, Proc. Roy. Soc. (London) **A217**, 9 (1953).
[14] D. E. Soule, Phys. Rev. **112**, 698 (1958).
[15] J. K. Galt, W. A. Yager, and H. W. Dail, Phys. Rev. **103**. 1586 (1956).
[16] P. N. Nozières, Phys. Rev. **109**, 1510 (1958).
[17] J. W. McClure, Phys. Rev. **112**, 715 (1958).
[18] J. W. McClure, Phys. Rev. **119**, 606 (1960).
[19] I. M. Lifshitz and A. M. Kosevich, Zh. Eksperim. i Teor. Fiz. **29**, 730 (1955) [English transl.: Soviet Phys.—JETP **2**, 636 (1956)].
[20] S. Titeica, Ann. Physik **22**, 129 (1935).
[21] B. Davydov and I. Pomeranchuk, J. Phys. (USSR) **2**, 147 (1940).
[22] G. E. Zilberman, Zh. Eksperim. i Teor. Fiz. **29**, 762 (1955) [English transl.: Soviet Phys.—JETP **2**, 650 (1956)].
[23] P. N. Argyres, Phys. Rev. **109**, 1115 (1958).
[24] I. M. Lifshitz, Phys. Chem. Solids **4**, 11 (1958).
[25] E. N. Adams and T. D. Holstein, Phys. Chem. Solids **10**, 254 (1959).

(hereafter referred to as AH) justified Titeica's method. At present, a number of calculations by different methods[26–30] also agree with Titeica's results. There is still some variation in the final formulas, however, depending upon the treatment of collision broadening[25] and the calculation of the transition probabilities.[31] The AH formulation is the most complete and most easily compared with experiment. In Sec. IV we show that their formulas give a very good description of the oscillations.

Although one might, in principle, apply the AH formulas to the total magnetoconductivity at all orientations, in this case there are considerable experimental and theoretical complications. Consequently, we applied the Landau relation to the magnetoresistivity data as a function of orientation. This method was satisfactory because our principal interest was in the determination of the individual electron and hole periods. The relationship between the two methods of analysis was established at the orientation $\theta=0°$. This arrangement allowed a determination of the orbital effective masses from the temperature and magnetic field dependences of the oscillatory amplitudes for all orientations. The variations of the effective mass with orientation could be qualitatively correlated with the period behavior. The results of this analysis are also given in Sec. III.

Finally, the results are summarized and conclusions are presented in Sec. V.

II. EXPERIMENTAL PROCEDURE

The purified graphite single crystal used in this study, EP-14, was described previously.[14] Also, the dc methods used in measuring the galvanomagnetic properties were essentially the same and the current, usually about 1 mA except at the highest values of θ, was always directed along the basal plane perpendicular to the a axis. The usual magnetic field ranged from 4 to 24 kG and the temperature range was extended from 4.22 down to 1.22°K by pumping over the liquid helium with a Kinney KDH-130 pump. Mercury and octoil "S" manometers were used for the vapor pressure determination and the error in the temperature was considered to be ± 0.01°K when operating below the lambda point. A Moseley X-Y recorder was employed to record the oscillatory curves, where the Y axis was proportional to the voltage drop due to the magnetoresistance V_ρ, or the Hall voltage V_H, and the X axis was proportional to the magnetic field H, measured by a rotating coil fluxmeter. These axes were calibrated against a Leeds and Northrup K-2 potentiometer and proton resonance, respectively. During the course of the study, over 180 curves were recorded.

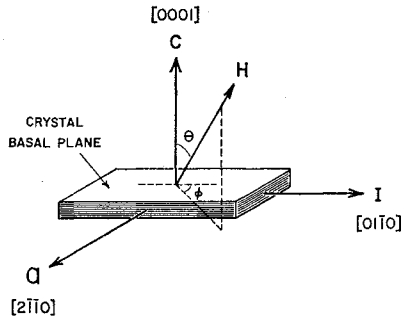

FIG. 1. Relative orientation of crystallographic axes with respect to the magnetic field **H** and the current **I**. The transverse magnetic field rotation scheme consists of rotating **H** from a direction parallel to [0001] to the direction [2$\bar{1}\bar{1}$0], keeping the aximuthal angle $\phi=90°$; whereas in the transverse-to-longitudinal rotation scheme, **H** starts from the same initial position and rotates to the direction [01$\bar{1}$0], keeping $\phi=0°$.

The period as a function of orientation was studied by using two magnetic field rotation schemes (see Fig. 1). The first consists of rotating **H** from a direction parallel to the c axis [0001], to the current direction **I** [01$\bar{1}$0], keeping the azimuthal angle $\phi=0$. This is called the transverse-to-longitudinal rotation scheme. Starting from the same initial direction in the second or transverse rotation scheme, H is rotated down to the a axis [2$\bar{1}\bar{1}$0], remaining always transverse keeping $\phi=90°$. In this investigation, the emphasis was on the large variation of the periods observed while rotating **H** through the angle θ. Of secondary interest was the variation obtained while rotating **H** azimuthally through the angle ϕ about the c axis for a particular value of θ. This aspect will be discussed at more length in the next section.

The mapping of the Fermi surface can be carried out with the magnetoresistance as with the susceptibility for although the nonoscillatory component depends on the rotation scheme, the oscillatory period is independent of the direction of **I**, depending only on the orientation of **H** with respect to the crystallographic axes.

Locating accurately the position of $\theta=90°$ was important in the process of running each set of orientation curves on the recorder. While previously the maximum of the magnetoresistance as a function of θ occurring at 0° was used as the criterion for alignment of **H** parallel to the c axis, it was found that the minimum at 90° in the nonoscillatory component proved to be far superior, being extremely sharp at low temperatures. The precision error using this procedure could be kept $\leq 0.2°$. The problem then remained to relate this observed minimum to the actual alignment of **H** with respect to the crystallographic axes for the Shubnikov-de Haas effect. This can be demonstrated by considering the two magnetic field rotation schemes used where, for

[26] R. Kubo, H. Hasegawa, and N. Hashitsume, J. Phys. Soc. Japan 14, 56 (1959).
[27] P. N. Argyres and L. M. Roth, Phys. Chem. Solids 12, 89 (1959).
[28] P. N. Argyres, Phys. Rev. 117, 315 (1960).
[29] A. M. Kosevich and V. V. Andreev, Zh. Eksperim. i Teor. Fiz. 38, 882 (1960) [English transl.: Soviet Phys.—JETP 11, 637 (1960)].
[30] V. G. Skobov, Zh. Eksperim. i Teor. Fiz. 38, 1304 (1960) [English transl.: Soviet Phys.—JETP 11, 941 (1960)].
[31] A. H. Kahn, Phys. Rev. 119, 1189 (1960).

the purpose of a simplified initial example, isotropy will be assumed. For the transverse-to-longitudinal rotation scheme, the position of the effective minimum in the nonoscillatory longitudinal magnetoresistance is not necessarily exactly the same as the minimum observed in the period of the oscillatory component, since the former occurs at the nearest approach of **H**||**I**, whereas the latter, being independent of the direction of **I**, occurs when **H** is actually parallel to the basal plane. As a result, for the isotropic case the overall alignment error for this rotation scheme would be $\leq 0.3°$. However, the high anisotropy of graphite reduces this error still further. In the transverse case, this error does not enter even in principle due to the fact that the nonoscillatory magnetoresistance minimum occurs when **H** is parallel to the basal plane which is identical to the case of the oscillatory component. Accordingly, because of this factor and an additional advantage due to the geometrical restriction of the sample mount in the Dewar, the latter rotation scheme was used for most of the orientation studies.

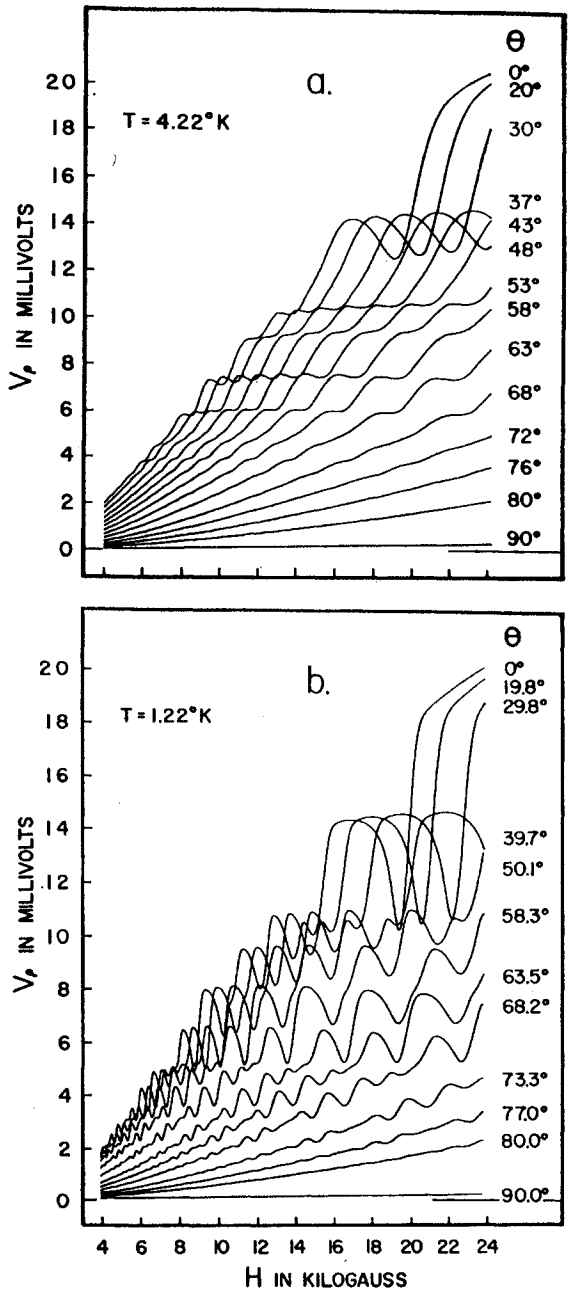

FIG. 2. Typical direct X-Y recorder traces of the measured voltage V_ρ (proportional to the magnetoresistance) versus magnetic field at 4.22°K (curves a) and at 1.22°K (curves b) for various orientation angles θ from 0 to 90°. The ordinate scale has been normalized for a current of 10 mA.

Another consideration, of course, is that with such a delicate crystal mounting, the Lorentz force might be sufficient to shift the crystal. This force would be of particular importance for the $\theta = 90°$ case. However, not only is the maximum force about 25 dyn, but its direction is such as to shift the crystal toward or away from the quartz mounting plate rather than to apply an unwanted torque about the crystal's transverse or longitudinal axis resulting in an erroneous evaluation of θ. The proof of these statements lies in the behavior of the actual crystal *in situo*, which is considered further in Sec. III.

One of the main problems in this study resulting from graphite's extreme anisotropy was the rapid decrease of the oscillatory amplitude as the crystal was rotated toward $\theta = 90°$. In fact, whether one could detect oscillations at all at this orientation was a critical factor in determining whether the Fermi surface was open or closed. Consequently, though the oscillations could be detected down to about 83° by conventional means, an auxiliary method was required to extend the detectability from 83 to 90°. It was found that the magnetic field dependence of the Hall voltage of an InSb crystal placed in the magnetic field in close proximity to the graphite crystal and stabilized at ice temperature had a behavior similar to the low-temperature nonoscillatory magnetoresistance component of the graphite. This device was then used as a bucking voltage source to compensate for almost all of the latter's nonoscillatory signal. The difference could then be amplified and presented on the recorder. By this means, the sensitivity could be enhanced by at least two orders of magnitude and small voltage differences of $<10^{-7}$ V could be detected. With this arrangement, oscillations were seen at $\theta = 90°$ with a signal-to-noise ratio of about 3:1.

III. PERIOD AND AMPLITUDE ORIENTATION BEHAVIOR

Typical magnetoresistance curves versus magnetic field are shown in Fig. 2. They were taken at orientation angles θ from 0 to 90° and at temperatures of 4.22 and 1.22°K. The increased amplitude and enhanced structure of the oscillations at the lower temperature is clearly evident. Also, it will be noted that the amplitude

falls off rapidly with increasing θ. This fact is shown clearly in Fig. 3. This very strong dependence is due to graphite's extreme orbital mass anisotropy causing a sharp decrease in the thermal damping factor of Eq. (1.2). Experimentally, this condition posed a severe problem of detection at high values of θ, as discussed in the previous section.

Another principal feature of the curves in Fig. 2 is the interference structure of two oscillatory terms, one due to majority electrons and the other to majority holes. Since the ratio of their periods is about $\frac{3}{4}$, the separation of terms is a tedious procedure.[8] For this reason, and because we wanted to extract additional information, an IBM 7090 was programmed to make a least-squares fit of the experimental data to a "generalized Landau relation." This formula gives for the oscillatory term due to the ith carrier

$$G_i(r)=H^n\sum_{r=1}^{\infty}W_i(r)\Omega(ru_i)\times\exp(-\lambda_i r)\cos[2\pi r s_i-\psi_i(r)], \quad (3.1)$$

where $s_i=1/P_iH$, $\lambda_i=u_i\Delta T_i/T=2\pi^2k\Delta T_i/\Delta E_i$, and where u and Ω are defined by Eq. (1.2). The quantity ΔT is the effective change in temperature due to collision broadening[32] given by

$$\Delta T=\hbar/(\pi k\tau_{\rm col}), \quad (3.2)$$

where $\tau_{\rm col}$ is the collision time. The formula coincides with the simple susceptibility theory[3] if $n=-\frac{1}{2}$, $W_i(r)=W_i(1)r^{-3/2}\cos(r\pi m_i^*/m_0)$ and $\psi_i(r)=(r+\frac{3}{4})\pi$. The generalization consists of letting n, the W's, and the ψ's have arbitrary values. This formula then can approximately reproduce most of the results of the various theories of the Shubnikov-de Haas effect. The computer program represents the effects of two carriers, including the fundamental and first harmonic ($r=1,2$) of each. For fixed n and ΔT's, the program varied the P's, m^*'s, W's, and ψ's to obtain the least value of the weighted sum of squares of deviations between the theory and experiment. The manner in which the values of n and the ΔT's were chosen will be discussed later.

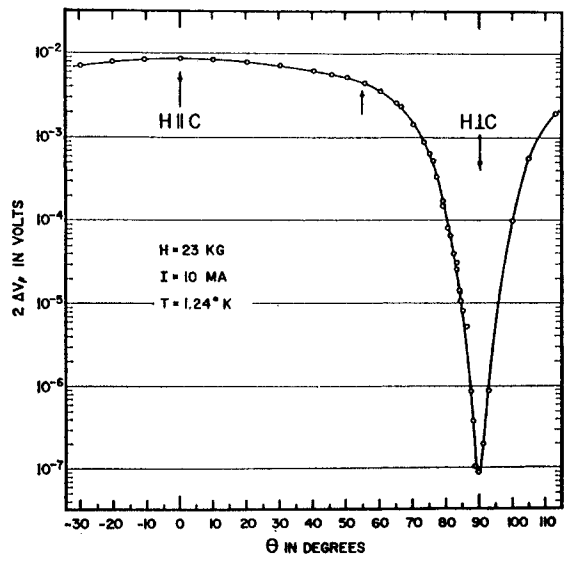

FIG. 3. Observed dependence of the oscillatory amplitude upon orientation at 1.24°K and 23 kG, normalized for a current of 10 mA. The arrow at $\theta=55°$ represents the approximate limit of Shoenberg's observations.

[32] R. B. Dingle, Proc. Roy. Soc. (London) **A211**, 517 (1952).

One of the important practical problems in the fitting concerned the statistical weighting of the data. If Eq. (3.1) described the phenomena exactly, the deviations would be expected to be random; however, the best reproduction of the positions of the maxima and minima was obtained when the average deviations were made proportional to the average amplitude of the oscillations.

The least-squares analysis can be applied either to the oscillations in the measured resistivity or to those of the measured conductivity. For purposes of analysis, the latter is preferred, since it more closely approximates the magnetoconductivity, for which the theory discussed in Sec. IV applies. The set of curves shown in Fig. 4(a) shows the oscillations in the resistivity for the transverse-to-longitudinal rotation scheme at 4.2°K. The shift to higher fields with increasing θ of a particular "destructive interference region" is indicated by arrows. In Fig. 4(b) are shown the oscillations in the conductivity for the transverse rotation scheme at 1.23°K, where the increased amplitude and structure of the oscillations are evident. Failure of the theory to fit these curves exactly is due mainly to the fact that the theoretical expression contains only two terms of the harmonic series, whereas more terms are important at the lower temperature.

A second method for isolating the electron term involves an analysis of the "low-field" region.[8] Equations (1.2) and (3.1) show that the oscillatory amplitude decreases with decreasing magnetic field and with increasing effective mass. The hole mass is larger than the electron mass (about twice at $\theta=0°$), causing the rate of damping of its term with decreasing H to be greater than for the electron term. At a sufficiently low magnetic field, only the electron term remains. Because of the increase of the effective masses with increasing θ, the upper limit of this "low-field" region progresses to higher fields, covering an ever larger portion of the observed field region, as seen in Fig. 4. Eventually at $\theta\geq 84°$, only the electron term could be observed reliably, although traces of interference structure were observed in some cases as high as 87°. A typical low-field curve is given in Fig. 5 showing the single electron term. By observing just this "low-field" region, the electron period was also determined at lower values of θ and was found to be in agreement with the results of the least-squares analysis. The derived periods are within 1.7% throughout the region of comparison.

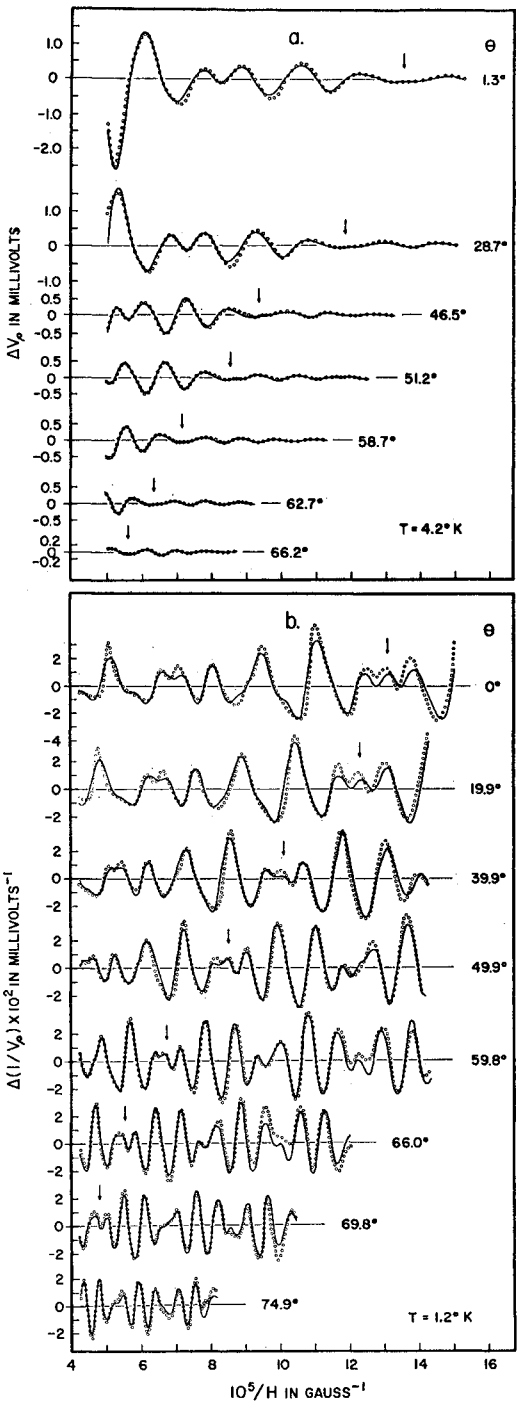

FIG. 4. Oscillatory components of the magnetoresistivity for the transverse-to-longitudinal magnetic field rotation scheme at 4.2°K (curves a) and of the measured conductivity (inverse resistivity) for the transverse scheme at 1.2°K (curves b) for values of θ from 0 to 75°. The voltages (proportional to the resistivity) are normalized for a current of 10 mA. The solid curves are fitted by least-squares using the Landau relation Eq. (3.1).

The over-all orientation behaviors of the individual electron and hole periods are shown in Fig. 6. Data for both rotation schemes and for eight temperatures between 1.2 and 4.2°K are included. Also, a comparison is made between the least-squares value and those found by the "low-field" method. This figure demonstrates the extreme anisotropy of graphite where, for instance, the electron period drops from $(2.07\pm0.04)\times10^{-5}$ G^{-1} at $\theta=0°$ to $(0.15\pm0.03)\times10^{-5}$ G^{-1} at 90°. The very existence of an oscillatory term for **H** in the basal plane (electron orbit in a plane containing the c axis) proves that the electron Fermi surface is *closed*. On the other hand, since the hole period which at $\theta=0°$ is $(1.51\pm0.03)\times10^{-5}$ G^{-1} was not observed at 90°, we cannot make so strong a statement about the hole Fermi surface. However, it will be shown below that it also is closed.

A. Electron Fermi Surface

It is possible to analyze the shape of the Fermi surfaces in some detail since the relative period values are of sufficient precision. The electron Fermi surface to a first approximation is an ellipsoid of revolution about the c axis. To determine the electron anisotropy ratio X_1 for the best ellipsoid, the measured $P_1(\theta)$ values in the range between 80 and 100° were used. For each $P_1(\theta)$, a X_1 was calculated giving an average electron Fermi surface anisotropy of $X_1=12.1\pm1.4$, predicting a most probable electron period at $\theta=90°$ of $(0.17\pm0.02)\times10^{-5}$ G^{-1}. The solid curve in Fig. 6 is for a true ellipsoidal Fermi surface with this anisotropy. To show this fit more clearly, the deviation from the true ellipsoid is

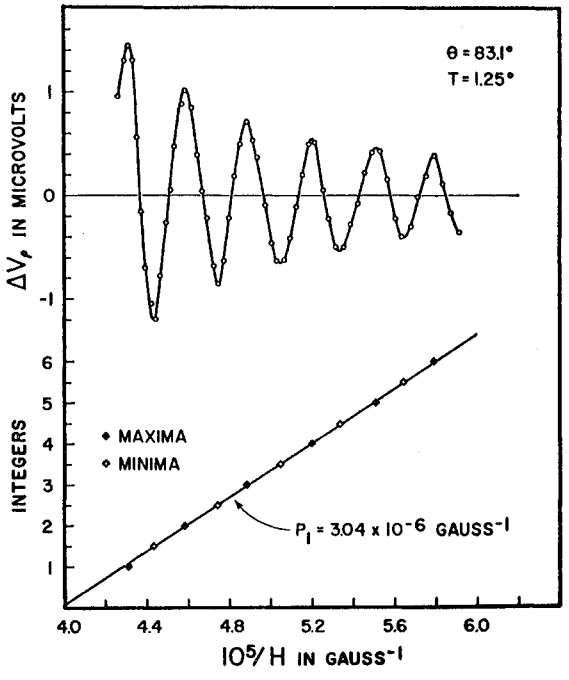

FIG. 5. Low-field oscillatory component of the magnetoresistance versus inverse magnetic field at $\theta=83.1°$ and $T=1.25°K$, normalized for a current of 10 mA. The integer plot is linear showing the absence of the hole term and gives a value of $3.04\pm0.07\times10^{-6}$ G^{-1} for the electron period at this angle.

given at the top of Fig. 7, showing it to be within $\pm 3\%$ over most of the range. Although there appears to be a slight "dumbbell-like" protrusion ($\sim 2.5\%$) occurring at θ between 25 and 60°, its reality is doubtful considering the scatter of points, as well as being a negligible effect on this highly elongated surface. Around 90°, the scatter is considerably larger ($\sim 10\%$) precluding any reliable statement about the exact shape of the actual electron Fermi surface tip.

The variation of the Fermi surface shape about the c axis was very difficult to resolve since the period behavior of these highly elongated surfaces approximates the cylindrical behavior $A\cos\theta$ regardless of the azimuthal angle ϕ and the shape of the cross section of the cylinder A. To obtain an approximate idea of the behavior of the period due to trigonal anisotropy, let us consider a rough model of the Fermi surface consisting of two pyramids with equilateral triangular bases placed back-to-back. The altitudes of the pyramids are parallel to the c axis and are ten times the length of a side of the base. The a axes are perpendicular to the base sides. The difference in the maximum cross sections cut by planes having perpendicular rotation axes corresponding to the transverse and transverse-to-longitudinal rotation schemes used experimentally is 2.5% at $\theta=60°$, 6.5% at 80°, and 14% at 90°. The observed period values for the two rotation schemes agreed to within $\sim 1\%$, relatively independent of θ, over the range for which they were compared, that is, out to 81° for the electron term and to 66° for the hole term. These results, then, would allow a small degree of trigonality, but somewhat less than that of the above extreme model.

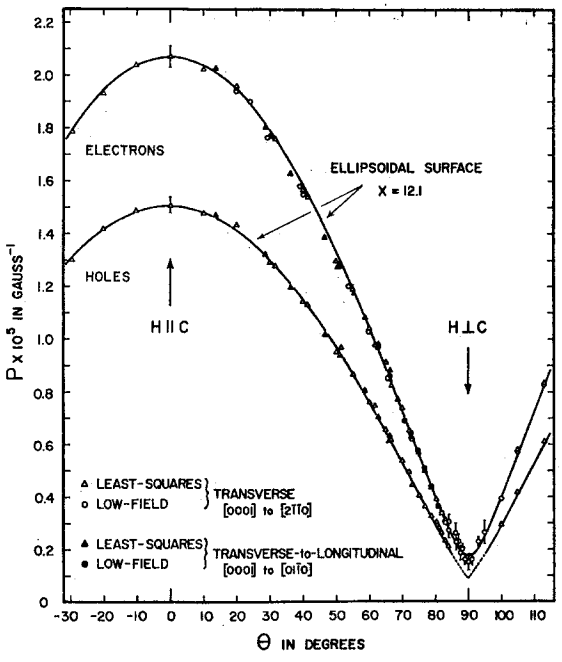

FIG. 6. Over-all dependence of the electron and hole periods upon orientation from $\theta=-30$ to $+113°$ for data taken in the range 1.2 to 4.2°K. Results from the transverse (open points) and the transverse-to-longitudinal (closed points) magnetic field rotation schemes are shown. These are subdivided into the results obtained from the least-squares and the low-field analyses. The solid curves represent the behavior of a Fermi surface having a true ellipsoidal shape with an anisotropy ratio of $X=12.1$. The dashed extrapolation of the hole curve from $\theta=85$ to 95° represents the behavior that would be expected for a hole surface with the extended conical tips (as shown in Fig. 8), and having an anisotropy ratio of 17.3. The error limits, for the sake of clarity, are shown only in certain representative regions; that is, the neighborhood of $\theta=90$, at 55, and at 0°.

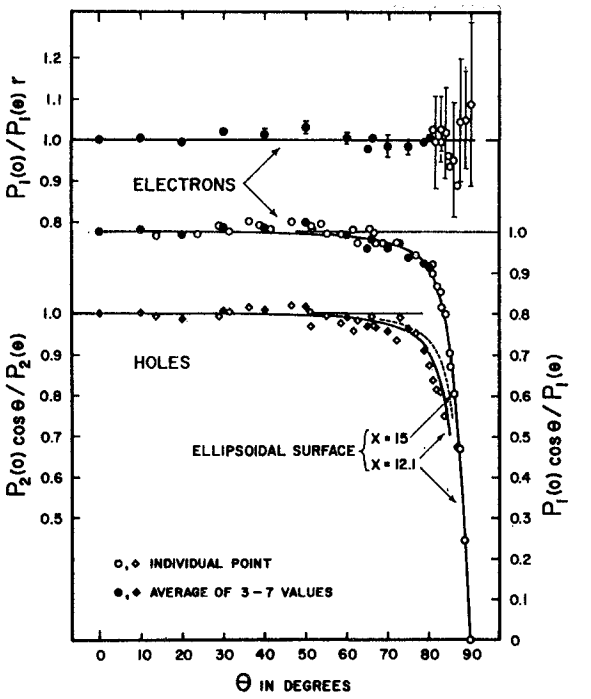

FIG. 7. Deviations of the electron and hole Fermi surfaces from a cylindrical surface shape (two lower curves) and the deviation of the electron Fermi surface from a true ellipsoidal surface shape having an anisotropy ratio of 12.1 (upper curve). The deviation from a cylinder is represented by $P_i(0)\cos\theta/P_i(\theta)$, where the P_i are measured periods for the ith type carrier. The curves represent the behavior of an ellipsoidal Fermi surface having an anisotropy ratio of $X=12.1$ (solid curve) and $X=15$ (dashed curve). The deviation of the electron surface from an ellipsoid is given by $P_1(0)/P_1(\theta)r$ where $r=[\cos^2\theta+X_1^{-2}\sin^2\theta]^{-1/2}$, the normalized radius vector to the ellipsoidal surface. The open points are individual measured values, whereas the closed points represent an average of 3 to 7 measured values.

Although the actual shape of the electron Fermi surface may differ some from the true ellipsoidal model, its volume should be very nearly equal to that of the ellipsoid. The carrier concentration N contained in the Fermi surfaces is then related to the observed oscillatory period by

$$N(\text{osc})=(\pi/3)(4e/\pi hc)^{3/2}XQP(0)^{-3/2}, \qquad (3.3)$$

where Q is the number of Fermi surfaces contained in the Brillouin zone. Previous results[14,17] obtained using the nonoscillatory galvanomagnetic data on the same sample studied here gave an average value for the elec-

tron concentration of $N_1(\text{nonosc})=(3.0\pm0.3)\times10^{18}$ cm^{-3}. If a value of $Q=4$ is chosen, then from Eq. (3.3), $N_1(\text{osc})=(2.90\pm0.35)\times10^{18}$ cm^{-3}. Such good agreement is experimental proof that there are *four* electron Fermi surfaces of each spin in the Brillouin zone. This result agrees with the theoretical result predicted by the parameterized SW model.[10]

B. Hole Fermi Surface

Although the hole oscillatory term could not be observed reliably for θ larger than 84°, its Fermi surface can be shown to be closed by the following arguments. The lower curves in Fig. 7 show the deviation of both the electron and hole surfaces from a cylinder. The ratio $P_2(0)\cos\theta/P_2(\theta)$ emphasizes the strong deviation of the surface inward, indicating that the hole Fermi surface is closed. In addition, the SW group-theoretical treatment predicts that if the electron surface is closed, the hole surface must also be closed.

As seen in Fig. 7, the hole period behavior can be fitted fairly well over the range it was measured by an ellipsoidal Fermi surface with an anisotropy ratio of 12, essentially the same as the electron surface. In fact, the ratio P_2/P_1 is remarkably constant[33] (0.730) with increasing θ. In addition, assuming that the electron and hole Fermi surfaces just fit into the Brillouin zone, the predicted hole surface anisotropy would be 12.3. Although this agreement seems plausible and supports previous theoretical estimates[10] of the Fermi surface sizes, the calculated value for $N_2(\text{osc})$ from Eq. (3.3), using the theoretical values of $Q=2$, is 2.2×10^{18} cm^{-3}; well below the previously determined[14,17] value of $N_2(\text{nonosc})=(2.8\pm0.3)\times10^{18}$ cm^{-3}. A discussion for the validity of assuming that there are two surfaces rather than three in the zone will be presented in Sec. V.

Since the actual period data cover only about 60% of the length of the hole Fermi surface, there is a reasonable latitude for adjustment of the shape of the ends. And, in view of the good agreement between the two types of carrier densities found for electrons, we have confidence in the nonoscillatory value for holes. Thus, the reverse procedure is taken starting by equating $N_2(\text{osc})$ to $N_2(\text{nonosc})$. A simple ellipsoidal surface satisfying this requirement would have an anisotropy ratio of 15. However, as shown in Fig. 7, the curve based on this anisotropy lies well outside of the observed points.

A composite model for the hole Fermi surface that overcomes the above difficulties to a large degree is one whose central section fits the 12.1 to 1 ellipsoid out to about 85° and which has a projection along k_z to accommodate the additional volume. A simple conical projection is considered that extends tangentially from the ellipsoid surface at 85°. This model gives a value of $N_2(\text{osc})=2.4\times10^{18}$ cm^{-3}, reducing the discrepancy

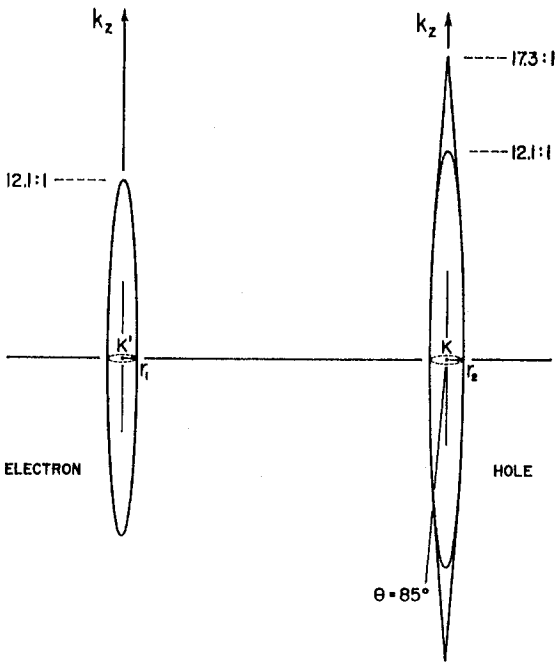

FIG. 8. Individual electron and hole Fermi surfaces determined from the θ variation. The electron surface has been completely determined experimentally while the hole surface has been determined experimentally to $\theta\simeq85°$. At 85° the proposed conical tip joins tangentially the 12.1:1 ellipsoid (dashed curve) to give an overall anisotropy ratio of 17.3. These surfaces are drawn to scale with the dimension along k_Z equal to 29.3×10^6 cm^{-1} for the electron surface and 49.2×10^6 cm^{-1} for the hole surface. The electron surface is centered at K' and the hole surface at K as shown in Fig. 13. Though the surfaces are drawn as figures of rotation about k_Z with maximum radii r_1 and r_2, the possibility of a small amount of trigonal asymmetry is discussed in the text.

with the $N_2(\text{nonosc})$ value to 14%, which may be reasonable in the light of all of the uncertainties. This hole surface has an anisotropy ratio of 17.3. Such a model resembles that predicted by theoretical calculations having an almost "diamond-shaped" Fermi surface.[34] It is worth pointing out that the theory predicts that the departure from rotational symmetry about the c axis is greater for the hole than for the electron surface and this fact should have a bearing on these shape and volume determinations. The individual derived Fermi surfaces are shown in Fig. 8, where they are drawn to scale to demonstrate the extreme anisotropies involved.

C. Orbital Masses

The computer results give effective orbital masses determined from fitting the magnetic field dependence of the amplitude of the oscillations at a fixed temperature; called the "field dependence effective masses." Since it is assumed throughout, of course, that ΔT is independent of temperature,[35] the correct values of ΔT

[33] In the present work each period was determined independently. In previous work (Refs. 6 and 8), Fourier analysis gave a simple period ratio of $\frac{3}{4}$.

[34] See Fig. 3 of D. E. Soule and J. W. McClure, Phys. Chem. Solids **8**, 29 (1959).

[35] The zero-field resistivity (6×10^{-7} ohm-cm) is independent of temperature from 1.2 to 4.2°K.

for each carrier are those for which the "field dependence effective masses" are also temperature-independent. Actually, there was a scatter in the effective mass values found ($\lesssim 15\%$), so that the ΔT values were determined by the requirement that there be no systematic change of these masses with temperature. The ΔT values obtained are 0.8°K for electrons and 0.6°K for holes at all values of θ that were analyzed. Although these ΔT values depend on the choice of n, discussed in the next section, the effective mass values are rather insensitive to n.

An alternative method for finding the effective mass uses the temperature dependence of the amplitude; called the "temperature dependence effective mass." The effects of the two types of carriers had to be separated first by calculating the amplitude of the fundamental due to each carrier at each temperature. The magnetic field value was chosen in the middle of the range; for, even if the field dependence of the amplitude were incorrect, the average amplitude had to be nearly correct in order to reproduce the experimental curves. It is this fact which makes the "temperature dependence effective mass" more reliable than the "field dependence effective mass." Figure 9 shows a typical plot of the amplitude for the electron and hole terms versus temperature at $\theta=0°$.

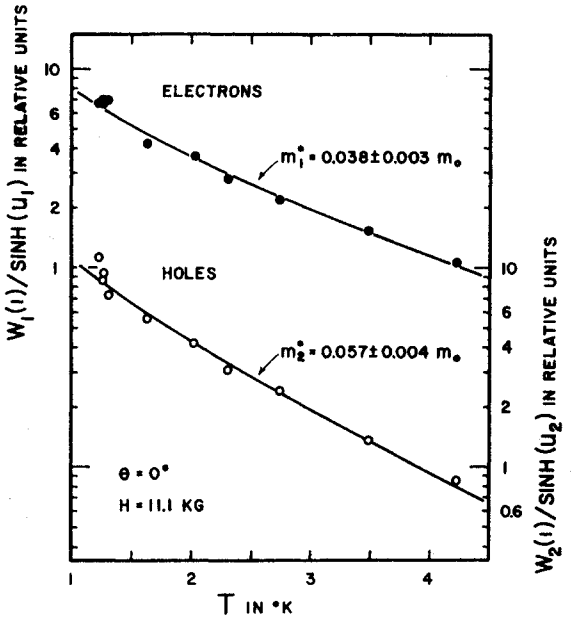

FIG. 9. Electron and hole effective orbital mass determinations from the temperature dependence of the amplitude. The ordinate is the amplitude of the fundamental oscillation in the inverse magnetoresistivity, divided by the absolute temperature, for a magnetic field of 11.1 kG parallel to the c axis. At each temperature, the points for each carrier were obtained from $W_i(1)/\sinh(u_i)$, $u_i = 2\pi^2 kTm_i^*c/heH$, where $W_i(1)$ and m_i^* are the parameters for the best fit of the field-dependent data *at that temperature*. The field-dependent fits were to Eq. (3.1) with $n=-1.2$, and $\Delta T_1 = 0.8$°K and $\Delta T_2 = 0.6$°K. The curves are given by $W_i/\sinh(u_i)$, but with the temperature-independent values of W_i and m_i^* adjusted to give the best fit to the points. The best values of the effective orbital masses are indicated on the graph. The uncertainties given for the mass values represent the range of values for which a curve of the type used could give a reasonable fit to the points.

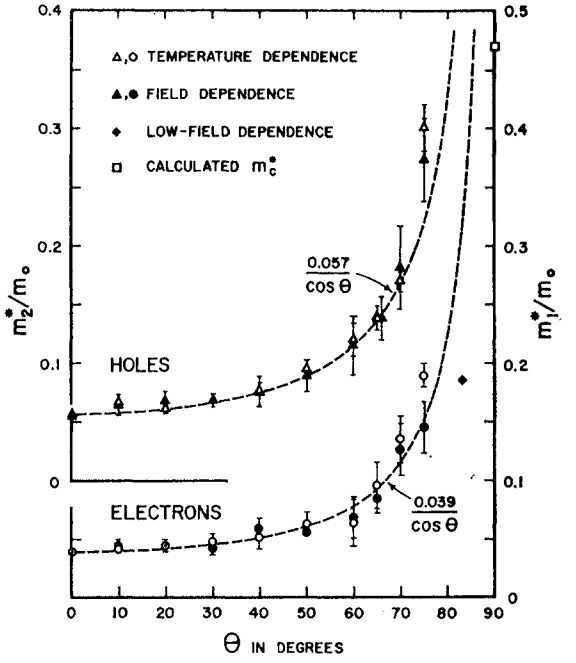

FIG. 10. Dependence on orientation of the effective orbital masses for electrons and holes, determined by two methods. The open symbols denote the "temperature dependence masses," determined as explained in Fig. 9. The solid symbols denote the average values for the "field dependence masses" determined by least-squares at various temperatures. The error limits represent the mean-square deviations. The values $n=-1.5$, $\Delta T_1 = 0.8$°K and $\Delta T_2 = 0.6$°K were used in the least-squares curve fits. The point at 83.1° was determined directly from the field dependence of the amplitude of the curve in Fig. 5. The dashed curves represent the orientation dependence of the orbital masses for a cylindrical Fermi surface parallel to the hexagonal axis. Up to $\theta=75°$, the curves deviate less than 5% from those for an ellipsoid with an anisotropy ratio of 12. The square symbol at $\theta=90°$ indicates the value of the electron cyclotron mass m_c^* predicted from the mass at $\theta=0°$ and the 12.1 anisotropy ratio.

Both types of effective masses as a function of orientation are shown in Fig. 10, where the points determined by the two methods agree to about 9% for electrons and 5% for holes. The dashed curves represent the behavior of the effective mass for a cylindrical Fermi surface which does not differ for $\theta \lesssim 70°$ from that for an ellipsoid with an anisotropy of 12 by more than the effective mass error. With the assumption that the Fermi surfaces are true ellipsoids having energies quadratic in wave number, the cyclotron mass becomes identical to the orbital mass observed here and so $m_{\|}^*/m_{\perp}^* = X^2$ and $m_c^* = (m_{\|}^* m_{\perp}^*)^{1/2}$, where $m_{\|}^*$ and $m_{\perp}^*$ are the effective masses parallel and perpendicular to the c axis and m_c^* is the cyclotron effective mass for the case where the magnetic field is perpendicular to the c axis. We find $m_{\|}^* = 5.7m_0$ and $m_c^* = 0.47m_0$ for electrons and $m_{\|}^* \approx 14m_0$ and $m_c^* \approx 0.9m_0$ for holes. The value of m_c^*

for electrons has also been plotted in Fig. 10, where an extrapolation to the lower curve seems reasonable.

IV. COMPARISON WITH THEORY

In this section, the AH theory[25] will be compared with the experimental results for the magnetoconductivity with the magnetic field parallel to the c axis ($\theta=0°$). The relation will then be established to the generalized Landau formula, which was used to analyze the magnetoresistivity at all orientations.

A. Adams-Holstein Theory

The results of AH apply to a simple electron-gas model in the high magnetic field limit. In this case, a high magnetic field is one for which $\omega\tau\gg1$, where $\omega=eH/m^*c$ is the cyclotron resonance frequency and τ is the relaxation time. Furthermore, we use the results of AH for point-impurity scattering (i.e., the potential of each scattering center is given by a Dirac delta function). We shall discuss the validity of these approximations below. The diagonal magnetoconductivity is given by AH as

$$\sigma_{xx}=\sigma_{cl}+\Delta\sigma_1+\Delta\sigma_2. \tag{4.1}$$

The quantity σ_{cl} is the classical high-field magnetoconductivity and is inversely proportional to the square of the magnetic field. This quantity is expressed as $\sigma_{cl}=Ne^2/m^*\omega^2\tau_{av}$, where τ_{av} is the average relaxation time, which does not depend upon the magnetic field. The $\Delta\sigma_1$ and $\Delta\sigma_2$ are quantum corrections which describe the Shubnikov-de Haas oscillations. As Adams and Holstein point out, $\Delta\sigma_1$ is due to transitions between the Landau level nearest the Fermi level and all other Landau levels, whereas $\Delta\sigma_2$ is due to transitions within the Landau level nearest the Fermi level. Except at very high magnetic field strengths, $\Delta\sigma_1$ dominates. In writing expressions for these quantities, it is useful to define a periodic "saw-tooth" function δ,

$$\delta=L+\tfrac{1}{2}-s, \quad 0\leq\delta\leq1, \tag{4.2}$$

where $s=1/PH$, and L is the largest integer which is less than or equal to $s-\frac{1}{2}$. For the absolute zero of temperature and no collision broadening, AH find to a very good approximation if $s>\frac{3}{2}$:

$$\Delta\sigma_1=(\tfrac{5}{2})s^{-1/2}\sigma_{cl}F, \tag{4.3a}$$

$$\Delta\sigma_2=(\tfrac{3}{2})s^{-1}\sigma_{cl}F^2, \tag{4.3b}$$

$$F=\tfrac{1}{2}\delta^{-1/2}-(\delta+\tfrac{1}{2})^{1/2}. \tag{4.3c}$$

Note that F is a periodic function of s.

The effect of temperature is easily introduced if the σ's are expressed as a harmonic series, by multiplying each term in the series by the factor Ω. The Fourier series for F is readily found, but that for F^2 does not exist, due to the δ^{-1} singularity. In order to circumvent this difficulty, AH introduced collision broadening. The result of broadening F with a simple Lorentz function is given by

$$F=\sum_{r=1}^{\infty}(2r)^{-1/2}e^{-\lambda r}\cos(2\pi r\delta-\tfrac{1}{4}\pi)\Omega(ru), \tag{4.4}$$

where λ and u are the same as in Eq. (3.1). One may also write $\lambda=2\pi/\omega\tau_{co1}$. The coefficient $(2r)^{-1/2}$ may be found by performing a Fourier series expansion of Eq. (4.3c), neglecting contributions less than about two percent of the coefficient. It has been obtained before by using the Poisson summation formula.[25] In the latter method, the coefficients are Fresnel integrals with upper limits depending upon s. To obtain Eq. (4.4), one must extend the upper limit to infinity. This condition appears to imply that Eq. (4.4) is good only for large s; but if one uses the asymptotic formulas for the Fresnel integrals, cancellations are found so that the error in (4.4) is less than 2% for s greater than $\frac{3}{2}$. The result also implies that the Landau formula for the susceptibility[3] is good for $s>\frac{3}{2}$ (i.e., for magnetic fields up to that of the last extremum), a fact which has previously been noted experimentally.[36] Equation (4.4) agrees with AH, except for an error of a factor of two in their paper. It also agrees with the result of Zilberman[22] (who gave only the first term in the series), with that of Skobov,[30] and with that of Kahn[31] (except for a multiplicative factor).

We treat $\Delta\sigma_2$ differently than AH, who applied collision broadening to F^2 and then found an approximate harmonic series. An examination of the theory leads us to believe that the density of states should be broadened prior to working out the conductivity. In the present case, this means that one should broaden F and then square the result. To reduce the square of Eq. (4.4) to a single harmonic series, it is necessary to perform some intermediate sums. We obtained approximate formulas for these sums by using the Euler-Maclarin sum formula.[37] We then adjust the constants in the formulas to obtain good agreement with a selection of exact values which were found numerically. The approximate result is

$$F^2\cong M+\sum_{r=1}^{\infty}e^{-\lambda r}[C_r\sin2\pi r\delta+D_r\cos2\pi r\delta]\Omega(ru), \tag{4.5a}$$

$$M=-\tfrac{1}{4}\ln(1-e^{-2\lambda}), \tag{4.5b}$$

$$C_1=0, \quad C_r=\tfrac{1}{4}(\pi-3r^{-1/2}), \quad r>1, \tag{4.5c}$$

$$D_r=\frac{e^{-2\lambda}}{2}\left\{\frac{a+b\lambda/(c+\lambda)}{(1+r)^{1/2}}+2\ln\left[\frac{(1+r+1/2\lambda)^{1/2}+(1+1/2\lambda)^{1/2}}{1+(1+r)^{1/2}}\right]\right\}, \tag{4.5d}$$

[36] J. S. Dhillon and D. Shoenberg, Phil. Trans. Roy. Soc. London **A248**, 1 (1955).

[37] E. T. Whittaker and G. N. Watson, *Modern Analysis* (Cambridge University Press, Cambridge, 1950), 4th ed., p. 127.

where $a=0.230$, $b=0.770$, and $c=0.763$. Formula (4.5d) holds for λ greater than about 0.2, which is adequate for the present case. With the correction of an error of a factor four, the AH result for the sine series is $C_r=\pi/4$ for all r. Our result for the cosine series is completely different from theirs. For a value of 0.25 for λ (which is about as small as that attained in the present data), D_1 is equal to 0.35. For this value of λ and the smallest value of s in the present data (about 2.5), the ratio of the amplitude of the fundamental term in $\Delta\sigma_2$ to that in $\Delta\sigma_1$ is about 0.1. Thus, $\Delta\sigma_2$ is not very important, especially for lower magnetic field strengths.

A set of sample theoretical curves are exhibited in Fig. 11. The curve for the case $T=\Delta T=0$ was calculated using Eqs. (4.3). The other curves were calculated by an LGP-30 electronic computer, using Eqs. (4.4) and (4.5). At each point, enough harmonics (the greatest number used was 14) were taken to give an accuracy of 0.02. Note that the peaks are extremely sharp and that the minima are more rounded. Note also that as the temperature decreases, the curves calculated from the harmonic series expansion approach the curve calculated from the simple formula (4.3c). The effect of the monotonic term M is interesting. If ΔT is small, M represents a quantum effect which is present even when the temperature is so high that the oscillations have damped out.

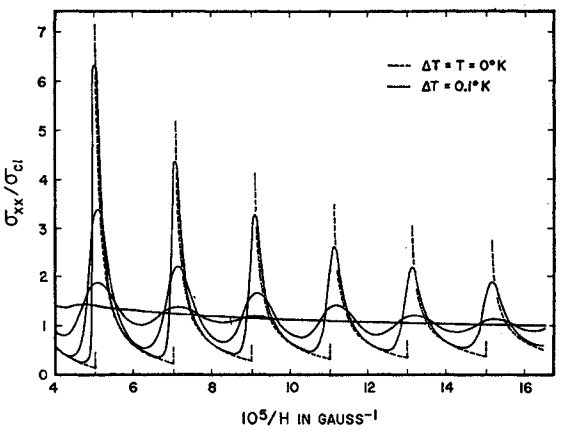

FIG. 11. Diagonal magnetoconductivity, calculated from the Adams-Holstein theory, as a function of inverse magnetic field strength. The solid curves are for temperatures of 1.26, 4.22, 10, and 20°K where the amplitude of oscillation decreases with increasing temperature. The dashed curve represents the unbroadened conductivity ($T=\Delta T=0$), which has infinite singularities. The curves were calculated for one carrier with the following parameters: $P=2\times10^{-5}$ G^{-1}, $m^*=0.04m_0$, and (except for the dashed curve) $\Delta T=0.1$°K.

B. Validity of the Theory for Graphite

We now examine the validity of applying these formulas to graphite. First we shall see if the condition $\omega\tau\gg1$ is obeyed. Analysis[17] of nonoscillatory data[14] on the same sample indicates that $\omega\tau$ is about equal to 100 at 20 kG. However, the AH theory gives a τ which oscillates as a function of magnetic field and, in the absence of collision broadening, is equal to zero at points where $\delta=0$. Near these points one may write $\tau\cong\tau_{av}(2s\delta)^{1/2}$, where τ_{av} is the value appropriate to the nonoscillatory phenomena (mobility, etc.). Following AH, we estimate the effect of collision broadening by replacing δ with $(\omega\tau)^{-1}$ in the above equation. This procedure gives an equation which can be solved for τ, yielding

$$\omega\tau_{min}\cong\omega\tau_{av}(2s/\omega\tau_{av})^{1/3}. \quad (4.6)$$

From (4.6) we estimate that the minimum $\omega\tau$ at 20 kG is about 37, and that at 5 kG, it is about 23. Thus, we see that the high-field approximation is adequate for the data reported here.

In our analysis we have treated τ_{col} as a constant, and have chosen its value to obtain the best fit to the experimental data. In the present data, which exhibits sharp peaks, the most important effect of the collision broadening is the reduction in amplitude of the peaks. Thus, the value of τ_{col} should be characteristic of the peaks, that is, it should be nearly equal to τ_{min}. The estimate given in the previous paragraph implies that the value of ΔT which gives the best fit to the present data may be as much as three times the value estimated using a τ_{av} obtained from the measured mobility. On the other hand, the peaks in the oscillatory susceptibility (de Haas-van Alphen effect) are not so sharp as those in the conductivity. The harmonic amplitudes in the susceptibility formula [see Eq. (3.1)] are proportional to $r^{-3/2}$, while those in the magnetoconductivity are proportional to $r^{-1/2}$ [see Eqs. (4.3) and (4.4)], which means that there are no singularities in the susceptibility even in the absence of collision broadening at absolute zero. Therefore, the value of τ_{col} which gives the best fit to the de Haas-van Alphen data should be closer to τ_{av}. This is in agreement with the experimental results, discussed below, where the value of ΔT [see Eq. (3.2)] found from Shubnikov-de Haas data is larger than the value found from de Haas-van Alphen data on the same sample.

We have neglected the variation with magnetic field of the Fermi level, the value of which is determined by the condition that the total number of electrons (or the number of electrons minus the number of holes) remains constant. Kahn and Frederikse[7] have calculated the change of the Fermi level at absolute zero for a single-carrier model. In Table I we give the location of the singularities in the density of states (which correspond to the singularities in the conductivity), according to their model. It is seen that the deviations from the ideal case (constant Fermi level) are appreciable. Two effects tend to reduce the variation in the present case: the simultaneous presence of electrons and holes, and the thermal damping. If the electrons and holes had identical effective mass tensors, and if their numbers were equal, the Fermi level would not change with magnetic field. Since the present case is not so sym-

TABLE I. Calculated positions of the singularities in the conductivity for simple models, taking into account the dependence of the Fermi level upon the magnetic field strength. The calculations are for a temperature of absolute zero and no collision broadening. The one-carrier results are from Kahn and Frederikse (Ref. 7). The two-carrier results are for twice as many electron (carrier 1) ellipsoids as hole (carrier 2) ellipsoids, for $2[m_{\parallel}^*(1)/m_{\parallel}^*(2)]^{1/2}=\frac{4}{3}$, and for $m_{\perp}^*(1)/m_{\perp}^*(2)=\frac{3}{4}$, so that $P_1/P_2=\frac{4}{3}$.

Index	Ideal	One-carrier	Two-carrier	
L	$1/PH$	$1/PH$	$1/P_1H$	$1/P_2H$
1	1.5	1.31	1.39	1.36
2	2.5	2.36	2.43	2.39
3	3.5	3.38	3.45	3.45
4	4.5	4.40	4.43	4.50
5	5.5	5.41	5.46	5.44
6	6.5	6.41	6.46	6.43

metric, we have calculated the positions of the singularities for a simple model in which the number of ellipsoids and the effective masses are approximately the same as in graphite, and in which the number of electrons and holes are equal. These results are also given in Table I. Note that the deviation from the ideal case is less than for the one-carrier model. The lowest quantum number peak we observe is the $L=2$ one for electrons, which is shifted about 3% from the ideal position. The effect of the finite temperature also reduces the Fermi level variation, so that the deviations in the actual experiment are of the order of, or less than, the experimental uncertainties.

As we have seen in the previous section, the energy band structure of graphite is very different from that of a free-electron gas with an isotropic effective mass. A fairly good approximation is a free-electron gas with an anisotropic effective mass: $m_{\parallel}$ parallel to the c axis and $m_{\perp}$ perpendicular to the c axis. The formulas given above would still apply when the magnetic field is parallel to the c axis; the only effect of the anisotropy would be to change the magnitudes of τ, N, and σ_{cl}. The anisotropy can have an effect on the shape of the oscillations for scattering potentials which have a finite range, as will be discussed below. As Adams and Keyes[38] point out, deviations from the effective mass model may be taken into account using the method of Lifshitz and Kosevich.[19] As far as fitting the data is concerned, the only change due to the latter effect would be to make the phase of the oscillations adjustable.

Another shortcoming of the formulas which we use is that they were derived for delta-function-potential scattering centers. The scattering potential actually has a finite range: That estimated for graphite by the Thomas-Fermi method[39] is 6A (the screening is isotropic in this approximation). This means that the scattering probability is reduced for changes of wave vector greater than about 0.2 of the Brillouin zone height. The case of scattering by screened Coulomb potentials was treated by AH for the electron gas model, but they did not carry the calculation through to formulas which can be used to fit experimental data. They concluded that the effect of introducing the finite range of the potential increases the strength of the δ^{-1} singularity relative to the $\delta^{-1/2}$ singularity. We have carried out detailed calculations for the anisotropic effective mass model with screened Coulomb scattering (the anisotropy simplifies the calculation) for a temperature of absolute zero and with no collision broadening. We find that the calculated σ_{xx}/σ_{cl} is very nearly the same as for the delta-function-potential case, except that the peaks are stronger. This result is in substantial agreement with AH. Since the temperature damping affects the peaks most strongly, the curves for the two cases should have the same shape except at very low temperatures. We have neglected the change of the range of the scattering potential as a function of the magnetic field strength, an effect which is very important in the extreme quantum limit and one which may also be important in the oscillatory range.

The AH theory treats the scattering in the Born approximation. Recently, Kahn[31] and Skobov[30] have treated the scattering exactly for the point scattering center. Their results indicate that the strong singularities in $\Delta\sigma_2$ are removed without resorting to collision broadening. Whether their formulation or that of AH is the most appropriate depends upon the strength of the collision broadening. We have not used their formulation, even though rough calculations indicate that we should, for two reasons: We wished to avoid the added complications in the analysis; and, since they have the same result as AH for $\Delta\sigma_1$, we believe that the results will not differ very much for the present data.

C. Comparison with Experiment

In order to compare the theory with the experimental results, we have calculated the experimental magnetoconductivity[40] $\sigma_{xx}=\sigma/[1+(R\sigma H)^2]$ from the conductivity σ and the Hall coefficient R, measured on the present sample at 1.26 and 4.22°K. The simple formula just given applies only when the magnetic field is parallel to the c axis ($\theta=0°$). Because of the fact that the contributions of the nearly equal numbers of electrons and holes cancel in pure graphite, the Hall coefficient is very small. Thus, the factor $R\sigma H$ is small and σ_{xx} is almost equal to σ, a result which we shall use later to simplify the analysis. This condition is in contrast to the one-carrier case (the only one explicitly considered by AH), in which $R\sigma H$ is very large, and σ_{xx} is inversely proportional to σ. In Fig. 12 we plot the experimental values of $H^2\sigma_{xx}$ against $1/H$ for two temperatures, 1.26 and 4.22°K. The quantity $H^2\sigma_{xx}$ would be a constant at

[38] E. N. Adams and R. W. Keyes, *Progress in Semiconductors* (Heywood and Company Ltd., London, 1962) Vol. VI, p. 85.
[39] N. H. March, Advan. Phys. 6, 1 (1957).
[40] J. M. Ziman, *Electrons and Phonons* (Oxford University Press, Oxford, 1960), pp. 487–494.

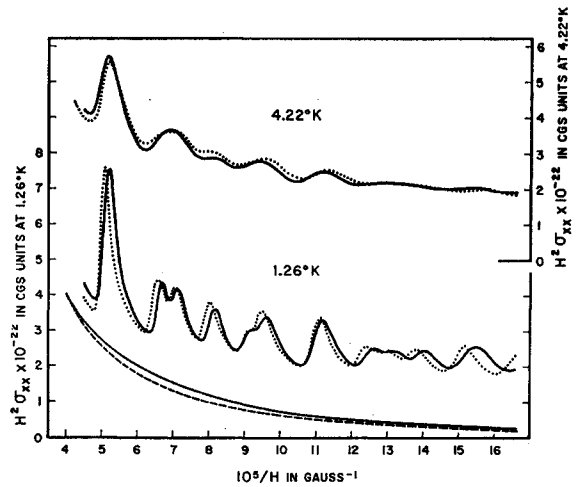

FIG. 12. Comparison of experimental and theoretical diagonal magnetoconductivities for the magnetic field parallel to the hexagonal axis at 4.22 and 1.26°K. The points represent the experimental data. The oscillating curves represent a linear combination of the Adams-Holstein theory and an empirical correction (same for both temperatures) represented by the monotonic solid curve. The parameter values in the Adams-Holstein calculations were chosen to give the best fit; the values are given in the text. The empirical correction is approximated by the function $64/(10^5/H)^2$ which is plotted as the dashed curve. This correction function corresponds to a constant term in σ_{xx} of 6.4×10^{13} cgs units, which is 0.004% of the zero-field value of σ_{xx}.

high magnetic field strengths if the behavior were classical. However, the actual curves differ from the classical behavior in two ways: There are oscillations; and the mid-line of the oscillations monotonically increases with increasing magnetic field strength (decreasing $1/H$). The latter effect is not contained in the AH theory; we represent it empirically by a monotonic function which approaches zero for small magnetic field strengths. The empirical function, which is shown in Fig. 12, will be discussed later in this section.

The corrected curve (which we may think of as the classical part plus the oscillations) was fitted with a linear combination of two theoretical functions (to represent the contributions of electrons and holes):

$$(H^2\sigma_{xx})_{\text{theo}} = B_1\sigma[{}_{xx}(1)/\sigma_{\text{cl}}(1)]+B_2[\sigma_{xx}(2)/\sigma_{\text{cl}}(2)], \quad (4.7)$$

where the indices 1 and 2 refer to electrons and holes, respectively, and $\sigma_{xx}(1)/\sigma_{\text{cl}}(1)$ stands for the AH expression for the ratio of the actual to the classical magnetoconductivity as a function of $1/H$ with the parameters P_1, m^*_1, and ΔT_1. A large number of curves for different values of the eight adjustable parameters (B, P, m^*, and ΔT for each carrier) were calculated and plotted by the computer. The best curves are plotted in Fig. 12 for the parameter values given below. Since the agreement between theory and experiment is not perfect, the selection of the "best" curves involves some subjective judgment. We concentrated upon the oscillations, attempting to reproduce the positions and relative amplitudes of maxima and minima and to obtain the correct dependence of over-all amplitude upon magnetic field and temperature. As might be expected, the values of the periods can be determined most accurately, a change of 10^{-7} G^{-1} in either period causing noticeable deviations from the experimental results. The uncertainties in the best values for the masses are about 5% and those in the ΔT's and B's are about 10%. These estimates are made on the assumption that the theoretical formula is exact; a change in the formula may cause parameter changes greater than these estimates.

It is seen that the agreement between the theoretical curves and the experimental results is very good. It is to be emphasized that the same parameter values are used at the two temperatures. It is also important to note that the AH theory gives the correct ratio of the amplitude of the oscillations to the low-field (say 15 kG) average magnetoconductivity. This fact alone would serve to confirm the AH theory, for the theories which disagreed with AH predict a much smaller amplitude of oscillation. Furthermore, we see that the shapes of the oscillations are reproduced remarkably well by the theory.

The most serious discrepancy is the monotonic increase in the mid-line with increasing magnetic field strength. The empirical correction functions used in Fig. 12 is approximately proportional to $(1/H)^{-2}$, which corresponds to a constant term in σ_{xx}. This effect was noticed in an earlier work,[17] where a few possible explanations were proposed. Another possibility is the variation of the range of the scattering potential with magnetic field strength. It has been shown[41] that taking this variation into account explains the fact that σ_{xx} is proportional to $1/H$ in the extreme quantum limit ($s\ll\frac{3}{2}$). The quantity $H^2\sigma_{xx}$ is then proportional to $(1/H)^{-1}$ in the quantum limit. It would be interesting to extend the calculation into the oscillatory region to see if it could explain the mid-line drift.

The parameter values found from the fit to the AH theory are quite reasonable. The values found for the periods are 2.02×10^{-5} G^{-1} and 1.47×10^{-5} G^{-1}. These values differ somewhat from the results discussed in Sec. III, mainly due to a small calibration error which was discovered after the AH calculations were completed. The effective mass values found are $0.040m_0$ for electrons and $0.058m_0$ for holes. A comparison of the effective mass values from several sources will be made below. The values of B_1 and B_2 are 0.66×10^{22} and 1.10×10^{22} cgs units, compared with 0.75×10^{22} and 0.60×10^{22} from the nonoscillatory analysis.[17] Although the agreement in the latter is not very close, there are many effects associated with the complexity of the band structure and the scattering mechanism which could account for the discrepancy.

We wish to give special attention to the values of the collision broadening parameters found, $\Delta T_1=0.80$°K

[41] J. W. McClure, Bull. Am. Phys. Soc. 7, 214 (1962).

and $\Delta T_2=0.56°K$. These values are in good accord with those found in Sec. III. The values of ΔT calculated using the nonoscillatory τ_{av} in the place of τ_{col} are 0.17° and 0.07°K, which are smaller than the values found here from curve-fitting by factors of five and eight, respectively. We saw above that τ_{col} should be less than τ_{av} (by about a factor three at 20 kG). This result is in the right direction to explain the discrepancy, but there is still not good quantitative agreement. However, the calculation of τ_{col} from τ_{av} was very approximate. Also, there is a distribution of relaxation times present even in the absence of a magnetic field, so that one should actually use the relaxation time for the states near the bulge of the Fermi surface for τ_{av}. Recent work by Bychkov[42] indicates that the effect of collision broadening on the de Haas-van Alphen effect is very complicated when $\omega\tau$ is greater than s and when δ is of the order of $(\omega\tau)^{-1}$, which is the case in the present work. In view of all these uncertainties, we feel that the agreement is not unsatisfactory, but believe that more theoretical work is desirable. It is worth pointing out that the agreement between the two methods of obtaining ΔT is much better for certain semiconductors which have spherical Fermi surfaces, and in which $\omega\tau$ is smaller than that for the present sample.[38]

The prediction that the ΔT values found from fitting Shubnikov-de Haas data are considerably larger than those found from fitting de Haas-van Alphen data is in agreement with the experimental facts. For a direct comparison, both the magnetoresistance and the susceptibility were measured on the *same* crystal by Berlincourt and Steele.[43] We have analyzed both sets of data.

TABLE II. Comparison of ΔT, the effective temperature shift due to collision broadening, from various sources.

Source	Method of determination	Electron ΔT_1	Hole ΔT_2
Present work	Fitting of Shubnikov-de Haas data.	0.80°K	0.56°K
Soule[a]	Collision time from carrier mobility.	0.17	0.07
Berlincourt and Steele[b]	Fitting of Shubnikov-de Haas data (present analysis).	3.0±1.0	
Berlincourt and Steele	Comparison of Shubnikov de Haas data to present Shubnikov-de Haas data.	3.6	3.4
Berlincourt and Steele	Fitting of de Haas-van Alphen data.	0.71	0.64
Shoenberg[c]	Fitting of de Haas-van Alphen data (his analysis)	1.5	0.9±0.6
Shoenberg	Fitting of de Haas-van Alphen data (present analysis).	0.5	0.6

[a] Reference 8.
[b] Reference 43.
[c] Reference 6.

[42] Y. Bychkov, Zh. Eksperim. i Teor. Fiz. **39**, 1401 (1960) [English transl.: Soviet Phys.—JETP **12**, 977 (1961)].
[43] T. G. Berlincourt and M. C. Steele, Phys. Rev. **98**, 956 (1955).

In their magnetoresistance curves, only one carrier (electron) is prominent. From an analysis of the temperature and magnetic field dependence of this data, a value of $\Delta T_1=3\pm1°K$ was obtained. In addition, both ΔT_1 and ΔT_2 may be estimated by the following qualitative argument.[8] The interference structure evident in their magnetoresistance data at 1.4°K is no stronger than that for our sample at 4.2°K. Thus, the quantity $T+\Delta T$ for their sample at 1.4°K should be greater than the same quantity for our sample at 4.2°K. This reasoning leads to estimates of $\Delta T_1\geq3.6°K$ and $\Delta T_2\geq3.4°K$ for the Shubnikov-de Haas effect in their sample.

These Shubnikov-de Haas values are about five times the values obtained by a least-squares analysis of the de Haas-van Alphen effect, $\Delta T_1=0.71°K$ and $\Delta T_2=0.64°K$. We have also analyzed Shoenberg's susceptibility data[6] in the same manner and obtained $\Delta T_1=0.5°K$ and $\Delta T_2=0.6°K$, compared with his estimates of 1.5 and 0.3 to 1.5°K, respectively. These values of ΔT are collected in Table II where they are grouped as derived from the Shubnikov-de Haas effect (upper half) or the de Haas-van Alphen effect (lower half).

D. Relation to the Generalized Landau Formula

We now discuss the relation between the analysis just presented and that using the generalized Landau formula. It is seen by comparison that the quantity $\Delta\sigma_1/\sigma_{c1}$ may be represented by taking $n=\frac{1}{2}$, $W_i(r)=W_i(1)r^{-1/2}$, and $\psi_i(r)=(r+\frac{1}{4})\pi$. Although the quantity $\Delta\sigma_2$ cannot be exactly represented in the Landau form, it is important only at high magnetic fields. The validity of this equivalence was verified by applying the least-squares analysis to test data calculated from the AH theory. The experimental magnetoconductivity was also subjected to the least-squares analysis. The results for the periods are in substantial agreement with those found from the magnetoresistivity. The effective masses were also in good agreement, as shown in Table III. The table also summarizes all of the present results for field and temperature dependence masses, as well as the results obtained by other authors.

Since this analysis was applied to the quantity $H^2\sigma_{xx}$, which has the same field dependence as σ_{xx}/σ_{c1}, the value of n chosen was $\frac{1}{2}$. For σ_{xx} alone, the value would be $-\frac{3}{2}$. The least-squares analysis for the magnetoconductivity in Sec. III was for $\sigma=1/\rho$, instead of σ_{xx}. The two differ by the factor $1+(R\sigma H)^2$, the maximum value of which was 1.1 in the data actually used. However, this factor varies very little with temperature and should not cause an error in the temperature dependence effective mass. However, it does vary with magnetic field by about 5% over the range of fields used; and so neglecting it could cause some error in the value of ΔT. Actually, good agreement was found both for the effective masses and for the ΔT's when the magnetic field was parallel to the c axis ($\theta=0°$). When the magnetic

TABLE III. Summary of effective mass values in the graphite layer plane. The adopted values are weighted averages of values found in the present work.

Source	Method of determination	Electron m_1^*/m_0	Hole m_2^*/m_0
Present work	Field dependence; magnetoresistivity	0.040	0.058
Present work	Temperature dependence; magnetoresistivity.	0.038	0.057
Present work	Field dependence; magnetoconductivity.	0.040	0.056
Present work	Temperature dependence; magnetoconductivity.	0.038	0.055
Present work	AH theory; magnetoconductivity.	0.040	0.058
Soule[a]	Field dependence; galvanomagnetic ratio.	0.030	0.060
Berlincourt	Field dependence; susceptibility	0.039	0.062
and Steele;[b] present work	Temperature dependence; susceptibility.	0.038	0.057
Shoenberg[c]	Temperature dependence; susceptibility; His analysis.	0.036	0.07
Shoenberg	Present analysis.	0.037	0.058
Nozières[d]	Cyclotron resonance; theory.	0.031	0.066
Inoue[e]	Cyclotron resonance; theory.	...	0.053
	Adopted values.	0.039±0.001	0.057±0.002

[a] Reference 8.
[b] Reference 43.
[c] Reference 6.
[d] Reference 16.
[e] M. Inoue, J. Phys. Soc. Japan **17**, 808 (1962).

field is not parallel to the c axis, considerable experimental work and numerical analysis would be necessary to obtain the experimental magnetoconductivity. However, since we wanted to obtain values only for the periods and effective masses, it was sufficient to use just the inverse resistivity.

Table III also includes the results of our least-squares analysis of the susceptibility data of Shoenberg and of Berlincourt and Steele. The adopted values of 0.039 m_0 for electrons and 0.057m_0 for holes, listed in the table along with their uncertainties, were chosen in order to include all of the different estimates made in the present work. The periods found from Shoenberg's data were 2.21×10^{-5} and 1.63×10^{-5} G^{-1}, in good agreement with his values of 2.20×10^{-5} and 1.65×10^{-5} G^{-1}. These values differ from those reported here, and Shoenberg[44] suspects that there was an error of a few percent in his magnet calibration. The periods found from Berlincourt and Steele's data are 2.12×10^{-5} and 1.57×10^{-5} G^{-1}, in fair agreement with those reported here. In addition, the absolute magnitude of the susceptibility parallel to the c axis is related to the curvature of the Fermi surface at the maximum cross section[19] (perpendicular to the c axis). This curvature can be expressed in terms of the anisotropy ratio of the ellipsoidal surface which coincides with the true Fermi surface at its "bulge," and is thus a rough estimate of the Fermi surface anisotropy. The anisotropy values found from Shoenberg's data are 10 for electrons and 15 for holes; those from Berlincourt and Steele's data are 11 for electrons and 18 for holes. These values are subject to considerable uncertainty, but are consistent with the anisotropies found in Sec. III.

[44] D. Shoenberg (private communication).

V. CONCLUSIONS

One of the main conclusions of this investigation is that the electron and hole Fermi surfaces in graphite are closed in *all* directions. These surfaces are, however, highly elongated in the direction of the hexagonal axis, and have anisotropy ratios of 12.1±1.4 for electrons and about 17 for holes. Although this result is based on a direct observation of the oscillatory term due to electrons throughout the angular range, the hole component could be resolved only to $\theta\simeq84°$. At this orientation, the hole term already showed a strong deviation away from a cylindrical surface. In addition, *both* oscillatory terms showed a *convex* surface variation about $\theta=0°$, whereas the Haering and Wallace model, with a corrugated cylindrical Fermi surface, would predict a *concave* behavior for the component with the largest period. The latter is the component we identify as being due to electrons and is the very term we see completely around to 90°. And further, the quite general SW band model requires that if the electron surface is closed, the hole surface must also be closed.

Inspection of the shape of these surfaces showed the electron surface (from θ variation) to be very close to a true ellipsoid, whereas the hole surface can be described more as "diamond-shaped," having pointed ends along the k_z axis. Cross sections from the azimuthal ϕ orientation were considerably more difficult to resolve. Although more indefinite, the present results do give sufficient information to allow a moderate degree of trigonal asymmetry.

Good agreement between the orbital effective masses derived from the dependence of the oscillatory amplitude on temperature and magnetic field substantiates a value of 0.039m_0 for electrons and 0.057m_0 for holes for motion in the basal plane. In addition, the variation of the orbital masses with θ is consistent with that ex-

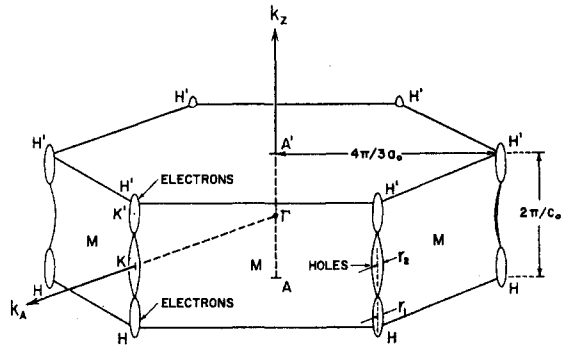

FIG. 13. The Brillouin zone for graphite, showing the placement of the electron and hole Fermi surfaces. The drawing is to scale, except that the lateral dimensions of the Fermi surfaces have been magnified by about a factor three. The center of the zone is denoted by Γ. The k_Z axis is parallel to the c axis (hexagonal axis) of the crystal, and the k_A direction is parallel to an a axis. The figure is a *superposition* of electron surfaces in the conduction bands and hole surfaces in the valence band. The degeneracy of the valence and conduction bands along the vertical zone edge HH' requires that the ends of the electron and hole surfaces touch as shown. The part of the electron Fermi surface which overlaps the horizontal faces is in the second conduction band, and is plotted in the second Brillouin zone. The degeneracy of the two conduction bands on the horizontal zone faces allows the overlapping part to be a smooth continuation of the main surface.

pected for the derived Fermi surfaces. All of the above conclusions rest entirely on the present experiment, except for the electron-hole identification, which depends on previous cyclotron resonance work. For a direct identification, however, a more satisfying and internally consistent procedure would be to observe the effect on the periods by shifting the Fermi level in a known way. This approach is now being investigated by controlled doping, using the acceptor boron.[45]

These Fermi surface anisotropies allow us to predict the anisotropy in the electrical conductivity. If we assume that the electron and hole relaxation times ($\tau_1=2.0\times10^{-13}$ sec and $\tau_2=3.4\times10^{-13}$ sec in the basal plane at 298°K)[17] are isotropic and constant over the Fermi surfaces and that $N_1\simeq N_2$, then the conductivity anisotropy ratio at room temperature is

$$\sigma_\perp/\sigma_{||}\simeq\left[\frac{\tau_1}{m_\perp^*(1)}+\frac{\tau_2}{m_\perp^*(2)}\right]\Big/\left[\frac{\tau_1}{m_{||}^*(1)}+\frac{\tau_2}{m_{||}^*(2)}\right]=190. \tag{5.1}$$

This value is in reasonable agreement with the best experimental ratio[46] of 110 to 175, considering the approximation of relaxation time isotropy and other uncertainties involved.

Comparison between the electron density N_1(nonosc) (total from all Fermi surfaces in the Brillouin zone) and N_1(osc)/Q (that due to one surface) definitely establishes that there are *four* electron Fermi surfaces in the Brillouin zone. From size and symmetry arguments, there are two possible locations for these surfaces in the reduced Brillouin zone shown in Fig. 13: (1e) all four aligned vertically along the center k_z axis between A and A', and (2e) aligned along the outer six zone edges HH', one-third of a surface at the top and one-third at the bottom as shown in the figure. Location (1e) is impossible on the basis of all band calculations[47] which agree that the energy of the conduction band at the center of the Brillouin zone, Γ, is about 10 eV *above* the energy at the zone edges. Thus, (2e) is taken as the accepted scheme.

For the hole Fermi surfaces, we assume initially that N_2(osc)$\simeq N_2$(nonosc). Due to the uncertainty in the anisotropy of these surfaces, values of $Q=2$ or 3 might be acceptable. For 2, one would find an N_2(osc) value 14 to 21% less than N_2(nonosc), whereas 3 results in a value of 18 to 29% greater than N_2(nonosc). A choice cannot be made, therefore, on this basis alone, and one must consider the most probable location of these surfaces. For two hole surfaces, two possible locations are (1h) both aligned along the central k_z axis between A and A', and (2h) aligned along the outer six zone edges HH', one-third of a surface at the middle as shown in the figure. For three surfaces, there are also two possible locations: (3h) all three aligned along the central k_z axis between A and A' and (4h) aligned vertically at the center of the vertical Brillouin zone faces, one-half a surface at each point M in the figure. Again, locations (1h) and (3h) are ruled out,[47] as with the electron case (1e), because the energy of the valence band at the center is 7 to 10 eV *below* the energy at the zone edge. The calculated[47] energy at point M is about 2 eV below the energy at the zone edge K so that possibly (4h) is also unlikely although the argument against it is not so strong as for the other cases. However, since group theory requires that the conduction and valence bands are degenerate along the vertical zone edges, and since the two electron Fermi surfaces were established above to be located along the zone edges with their combined lengths less than the zone height, then the hole surfaces also are located at the zone edges (location 2h) as shown in the figure. This result agrees with the parameterized SW model and represents that assumed in Sec. III in calculating the hole Fermi surface length. The Fermi surfaces as shown in Fig. 13 therefore represent the most probable configuration for graphite.

[45] D. E. Soule, *Proceedings of the Fifth Conference on Carbon* (Pergamon Press, Inc., New York, 1961), Vol. I, p. 13.
Note added in proof. Since this paper was written, de Haas-van Alphen measurements have been made on dilute boron-doped graphite crystals [D. E. Soule, I.B.M. J. Res. Develop. (to be published).] A preliminary analysis of the data supports the above identification of the two major oscillatory periods.

[46] W. Primak and L. H. Fuchs, Phys. Rev. **95**, 22 (1954); W. Primak, *ibid.* **103**, 544 (1956).

[47] See, for example, R. R. Haering and S. Mrozowski, *Progress in Semiconductors* (Heywood and Company Ltd., London, 1960), Vol. V, p. 273. The most accurate band calculation is by F. J. Corbato, *Proceedings of the Third Conference on Carbon* (Pergamon Press, Inc., New York, 1959), p. 173; and Quarterly Progress Report, Solid State and Molecular Theory Group, M.I.T. 1956, p. 23 (unpublished).

Knowing the Fermi surface positions, we can next consider quantitatively their size with respect to the reduced Brillouin zone. The maximum Fermi surface radii perpendicular to the c axis found from $P_1(0)$ and $P_2(0)$ using Eq. (1.1) are $r_1=1.21\pm0.02$ for electrons and $r_2=1.42\pm0.02$ for holes in units of 10^6 cm^{-1}. These are 0.72 and 0.84%, respectively, of the distance along k_A from a corner K to the center Γ of the zone, $4\pi/3a_0=170.3$. In the k_z direction, the height of the zone is $2\pi/c_0=93.6$, whereas the two electron surfaces have heights of 29.3 ± 3.4 each. Due to the degeneracy of the valence and conduction bands along the vertical zone edge, the hole surface tips abut the tips of the electron surfaces, as shown in the figure. Thus, with a hole surface height of about 49.2, the electron surfaces will overlap the top and bottom of the Brillouin zone by about 7.1.

This result provides a new and direct measure of Δ, which represents the difference in potential between the two types of sites for carbon atoms in the graphite lattice.[48] According to the parameterized SW model,[11,10] the relation between the value of k_z at the upper end of the hole Fermi surface and the Fermi energy ζ is given by

$$\Delta=\zeta+2\gamma_1\cos(c_0k_z/2), \tag{5.2}$$

where γ_1 is the nearest layer interaction integral. Then, using the well established values of 0.02 eV for the Fermi energy[6,8,10] and 0.30 eV for the γ_1 parameter,[49,18] we obtain

$$\Delta\simeq-0.12 \text{ eV}.$$

Previous estimates of this parameter have given values closer to zero, but these methods were more indirect.[48,10,18] Recently, however, another determination based on the temperature dependence of the g factor[50] gave a value of about -0.1 eV, in reasonable agreement with the above value.

As mentioned above, the azimuthal orientation results set a limit on the amount of departure from rotational symmetry about the c axis which the Fermi surfaces may have, a limit consistent with the available information. The band parameter which describes the departure from trigonal symmetry has been called γ_3. The simple tight-binding theory states[10] that γ_3 is nearly equal to another band parameter γ_4. A value of γ_4 has been found from analysis of the g-shift in the electron spin resonance,[50] which yielded a value of $\gamma_4=0.28$ eV. We have calculated the shapes of the cross sections, perpendicular to the c axis, of the Fermi surfaces for $\gamma_3=0.28$ eV. We find that the cross section of the electron surface resembles a triangle with rounded corners, as shown in Fig. 14. The radius vector varies as a function of the azimuthal angle ϕ by about $\pm16\%$. The deviation between the extremal periods at $\theta=90°$, as obtained from the two perpendicular magnetic field rotation axes, would be about 10%. The cross section of the hole surface is more distorted, resembling a triangle with rounded corners and with concave sides, as shown in Fig. 14. The azimuthal variation of the radius vector is about $\pm40\%$, and the deviation between the two extremal periods at $\theta=90°$ would be about 20%. The expected deviation between periods predicted for the two rotation schemes is less for electrons and greater for holes than those deduced from the simple triangular model discussed in Sec. III. This value for γ_3 would predict a deviation of approximately $\lesssim4.6\%$ for the electron surface at $\theta=80°$, compared with the observed deviation of $\sim1\%$. For the hole surface, the predicted deviation would be $\lesssim2.9\%$ at $\theta=60°$, compared with the observed deviation of $\sim1\%$. Although subject to considerable uncertainty, these results indicate that the actual Fermi surfaces are closer to rotational symmetry than the above γ_3 band model would predict, that is γ_3 must be considerably smaller than 0.28 eV. Very accurate data at the higher values of θ would be needed to determine the value of γ_3 reliably from the shape of the Fermi surfaces. Even so, this fact that γ_3 should be small has been substantiated by recent results obtained from magneto-optical reflection measurements,[51] where γ_3 was found to be 0.145 eV at 4.2°K.

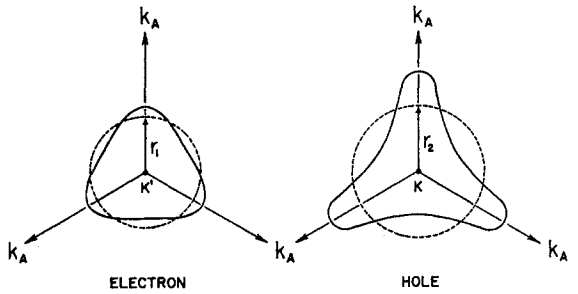

FIG. 14. Calculated maximum Fermi surface cross sections perpendicular to the hexagonal axis showing the trigonal asymmetry. The point K is at the center of the vertical Brillouin edge and the point K' is at a different place on the same edge (see Fig. 13). The lines marked k_A represent the Brillouin zone boundaries. The solid curves are calculated for $\gamma_3=0.28$ eV, and the dashed curves (circles) are for $\gamma_3=0$. Both sets of curves are to the same scale, with the values of the radii of the circles derived from the periods at $\theta=0°$ given by $r_1=1.21\pm0.02\times10^6$ cm^{-1} and $r_2=1.42\pm0.02\times10^6$ cm^{-1}. For each carrier the areas enclosed within the two curves are the same to within 1%.

The present work provides the most complete test to date of the Adams-Holstein theory. It is important that the AH theory correctly describes the amplitude of the oscillations, since the competing theories predict amplitudes which are very much smaller.[25] In addition, the AH theory reproduces the shape of the oscillations, which are so asymmetric and have such sharp cusps that many harmonics are needed for their description. Such a

[48] J. L. Carter and J. A. Krumhansl, J. Chem. Phys. **21**, 2238 (1953).
[49] Y. H. Ichikawa, Phys. Rev. **109**, 653 (1958).
[50] J. W. McClure and Y. Yafet, *Proceedings of the Fifth Conference on Carbon* (Pergamon Press, Inc., New York, 1962), Vol. I, p. 22.
[51] M. S. Dresselhaus and J. G. Mavroides (to be published).

fit to the oscillation shape verifies that the harmonic amplitudes are proportional to $r^{-1/2}$ and not to $r^{-3/2}$, as proposed by competing theories, which would give sharp *minima* in σ_{xx} instead of *maxima*.[25] There are, however, two important points of disagreement between the AH theory and our results. The first is the "mid-line drift" observed in σ_{xx}. Although there are several effects which could be responsible, we suspect that the dependence of the range of the scattering potential upon the magnetic field strength is most likely. The second point of disagreement is that the ΔT values (effective temperature shift due to collision broadening) found from curve-fitting the Shubnikov-de Haas data are several times greater than the ΔT values estimated using the conductivity relaxation time. Both of these points indicate that more theoretical work needs to be done on the details of the scattering process.

We have verified that the generalized Landau formula may be used to analyze Shubnikov-de Haas data for the periods, masses, and ΔT values. This fact was concluded theoretically, since the periodicity and the temperature dependence are the same for all theories of the Shubnikov-de Haas effect. The generalized Landau formula was tested experimentally by analyzing the magnetoconductivity data at $\theta=0°$ obtaining good agreement with the results of the analysis using the AH formula. Another simplification which was successfully tested on the data at $\theta=0°$ for the present case of graphite was the replacement of the magnetoconductivity by the measured conductivity (inverse of the measured resistivity). These two simplifications considerably reduced the work involved in taking data and performing the numerical analysis. Furthermore, use of the generalized Landau formula gave results which do not depend upon any specific theory.

The use of the least-squares method to analyze the data was, on the whole, successful. Results for the periods are in good agreement with those using the usual integer plot, which was used for the electron term in the low magnetic field region where the hole term is negligible. However, the least-squares method does have certain pitfalls. To obtain reliable results, extremely accurate magnetic field calibrations must be used and attention must be given to the statistical weighting scheme.

We have established that the ΔT values found from fitting Shubnikov-de Haas data may be considerably larger than those found from fitting de Haas-van Alphen data. It was also found from the ΔT's (and therefore the impurity concentration) for Berlincourt and Steele's sample are about four to five times those found in this work, showing the higher quality of the present sample. This was expected in view of a previous comparison of the nonoscillatory magnetoresistance results,[14] where the ratio of the average relaxation times was found to be about three.

ACKNOWLEDGMENTS

The authors would like to express their appreciation to Miss B. J. Vizi, C. W. Nezbeda, and R. P. Ulman for assistance during the course of the measurements, to Dr. E. N. Adams for several helpful conversations, and to Dr. D. Shoenberg, Dr. T. G. Berlincourt, and Dr. M. C. Steele for communicating their original data.